On the Maintenance of the Subtropical Front and its Associated Countercurrent[1]

BENOIT CUSHMAN-ROISIN

Mesoscale Air–Sea Interaction Group, The Florida State University, Tallahassee, FL 32306

(Manuscript received 31 October 1983, in final form 7 May 1984)

ABSTRACT

In the North Pacific and Atlantic Oceans, the Subtropical Countercurrent is an eastward flow across the Subtropical Gyre at a latitude where a classical wind-driven circulation theory would predict a westward flow. It is in geostrophic balance with the Subtropical Front, a zonal density front which runs across the ocean basin. From previous numerical models, it is argued that convergence of Ekman transports can hardly be the primary reason for the existence of such a phenomenon and that thermodynamic effects play a crucial role. To elucidate how these may be responsible for the frontal structure, a very simple analytical model is constructed where the dynamics yield motions consisting of a nondivergent wind-driven Sverdrup current and a geostrophic thermal flow that is divergent on a beta-plane. The surface temperature is governed by a nonlinear hyperbolic equation, for which the corresponding characteristics intersect, separating the basin into two distinct regions limited by a temperature discontinuity. We then show how the beta-plane convergence of the thermally driven flow is responsible for this frontal formation and how all consequent results such as location of front, temperature jump across it, flow pattern and vertical velocity compare favorably with observations and numerical models. Disagreement along the eastern boundary is recorded and explained by the absence of California Current dynamics in the present simple model. The conclusion is that, aside from convergence of Ekman transports, the convergence of the thermally driven flow on a beta-plane may be the primary mechanism responsible for forming and maintaining the Subtropical Front–Subtropical Countercurrent system.

1. Introduction

Much of the credit for the discovery and documentation of the Subtropical Front and Subtropical Countercurrent in the North Pacific Ocean must go to Japanese investigators. From calculations of the Sverdrup transport from wind-stress data during springtime, Yoshida and Kidokoro (1967a, 1967b) predicted the existence of an eastward current at a latitude of the Subtropical Gyre where one would otherwise expect a westward flow feeding the western boundary current. For this reason, they coined the name Subtropical Countercurrent. Later, Uda and Hasunuma (1969) confirmed such eastward flow from direct current-meter data as well as from geostrophic calculations based on hydrographic sections. The Subtropical Countercurrent is seen as a shallow, density-driven geostrophic flow ("thermal wind") associated with a Subtropical Front. The two features are two facets of a single phenomenon. Detailed charts of current directions in the western North Pacific prepared by Uda and Hasunuma (1969) prove clearly, in spite of some seasonal variations, the existence of an eastward current, significantly separated from the Kuroshio, that originates around 20°N and tilts slightly northward as it flows eastward.

A more recent update of observations in the western North Pacific is found in a paper by Hasunuma and Yoshida (1978). They presented a long-term mean geopotential anomaly which testifies to the existence of the Subtropical Countercurrent as a steady feature. Vertical density sections show that the shallow eastward current is associated with a density front, located around 18–20°N in the western North Pacific.

Observations of the Subtropical Front in the central and eastern North Pacific are reported by Roden (1972, 1975, 1980a and 1980b). In particular, large-scale satellite coverage (Fig. 1) shows that the Subtropical Front can be traced across almost the entire zonal extent of the North Pacific, tilting slightly northward toward the east. Near the American coast, the Subtropical Front joins the California Current front which is, however, of a different, coastal origin. Although satellite data are the only present source of ocean-wide, detailed coverage, the sea surface temperature that they provide may not accurately reflect subsurface conditions, and caution must be in order when one interprets Fig. 1. Kenyon (1981) independently concludes that a northeastward current exists in the eastern North Pacific. The Subtropical Front–Countercurrent system is thus a large-scale feature characterizing the entire ocean. In addition, Schroeder (1965) presented meridional sections of monthly temperatures in the North Atlantic Ocean. No essential difference is found between structure of the Subtrop-

[1] Contribution No. 203 of the Geophysical Fluid Dynamics Institute at The Florida State University.

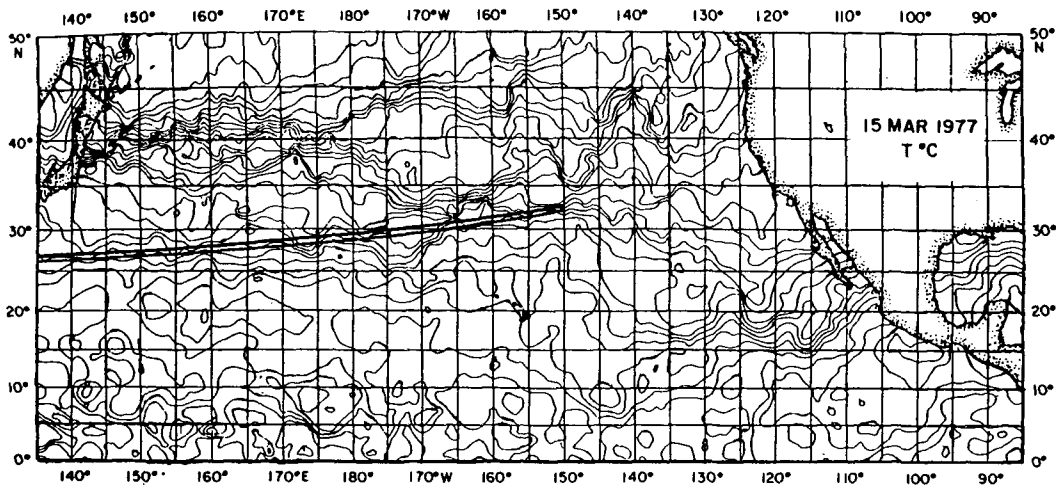

FIG. 1. Satellite map of sea surface temperature for 15 March 1977, based on Gosstcomp maps (National Environmental Satellite Service, 1977–78). (Adapted from Roden, 1980b.)

ical Front in the North Atlantic and that in the North Pacific. The phenomenon has, therefore, a very general character, and deserves full physical understanding. For simplicity, however, the present work focuses on the North Pacific Ocean only.

A very early hypothesis (and, in fact, the one that motivated the Japanese effort in documenting the Countercurrent) was that of Yoshida and Kidokoro (1967a, 1967b), who found that Sverdrup transport calculations lead to eastward currents in the middle of the Subtropical Gyre. This hypothesis is now rejected (Takeuchi, 1980) based on the fact that only springtime wind stresses lead to such currents while the Subtropical Countercurrent is a year-round feature.

A first model leading to an eastward current across the middle of the Subtropical Gyre was presented by Haney (1974). A crucial feature of that model is the combination of a dynamical forcing (surface wind stress) and thermodynamical forcing (surface heat flux with warming near the equator and cooling at high latitudes). This combination of forcings drives both wind-driven and thermal currents. The results show an eastward Countercurrent, whose shallowness suggests that it is of thermal origin. Haney's model demonstrates the importance of thermodynamically forced currents insofar as being comparable to wind-driven currents. However, as a result of the wide span covered by the model (50°S to 50°N), a lack of resolution precluded the representation of a zonal temperature front such as the Subtropical Front. More recently, Takeuchi (1980) modeled a smaller region (equator to 45°N) with essentially the same physics but with much more horizontal and vertical resolution. His numerical results clearly show a Subtropical Front–Countercurrent structure (Fig. 2). The current pattern basically consists of the classic wind-driven circulation, superimposed on which is an eastward thermal flow along the Subtropical Front. This feature is found in the upper hundred meters of the water column only. Below, the current pattern consists of the same wind-driven circulation but with an opposite thermal return flow. (As can be anticipated, baroclinic thermal currents have no vertical mean on a flat bottom.) In summary, the combination of surface wind stress (dynamical forcing) and surface heat flux (thermodynamical forcing) sets up a hybrid flow pattern consisting of a barotropic wind-driven circulation and a baroclinic thermally driven cell. But a question remains: Why do these two flow fields combine in such a way as to produce a large temperature gradient and a consequently narrow and vigorous thermal current? Where among all the physical processes is the frontogenetic mechanism?

To answer that question, the likelihood of frontogenesis solely by Ekman convergence is first investigated (Section 2). It is concluded that, although this source of convergence may strengthen the front, it cannot be the primary mechanism at work in the maintenance of the front. A minimal model retaining only the simplest physics (wind-driven circulation, thermal currents and temperature advection) is then constructed (Section 3). The dynamics are solved analytically, and the problem reduces to a single, nonlinear hyperbolic equation for the temperature at the base of the surface Ekman layer. This equation is then investigated in Section 4 to show how converging characteristics set up a frontal line and how the convergence of the meridional component of the thermal current on a beta-plane accounts for that structure. A numerical solution is also presented to quantify the results. Finally, qualitative examination of particle trajectories leads to the conclusion that the subtropical-gyre region is well-divided in two water masses, the tropical water to the south and the subtropical water to the north of the front. A verbal recapitulation of the frontogenetic mechanism and of

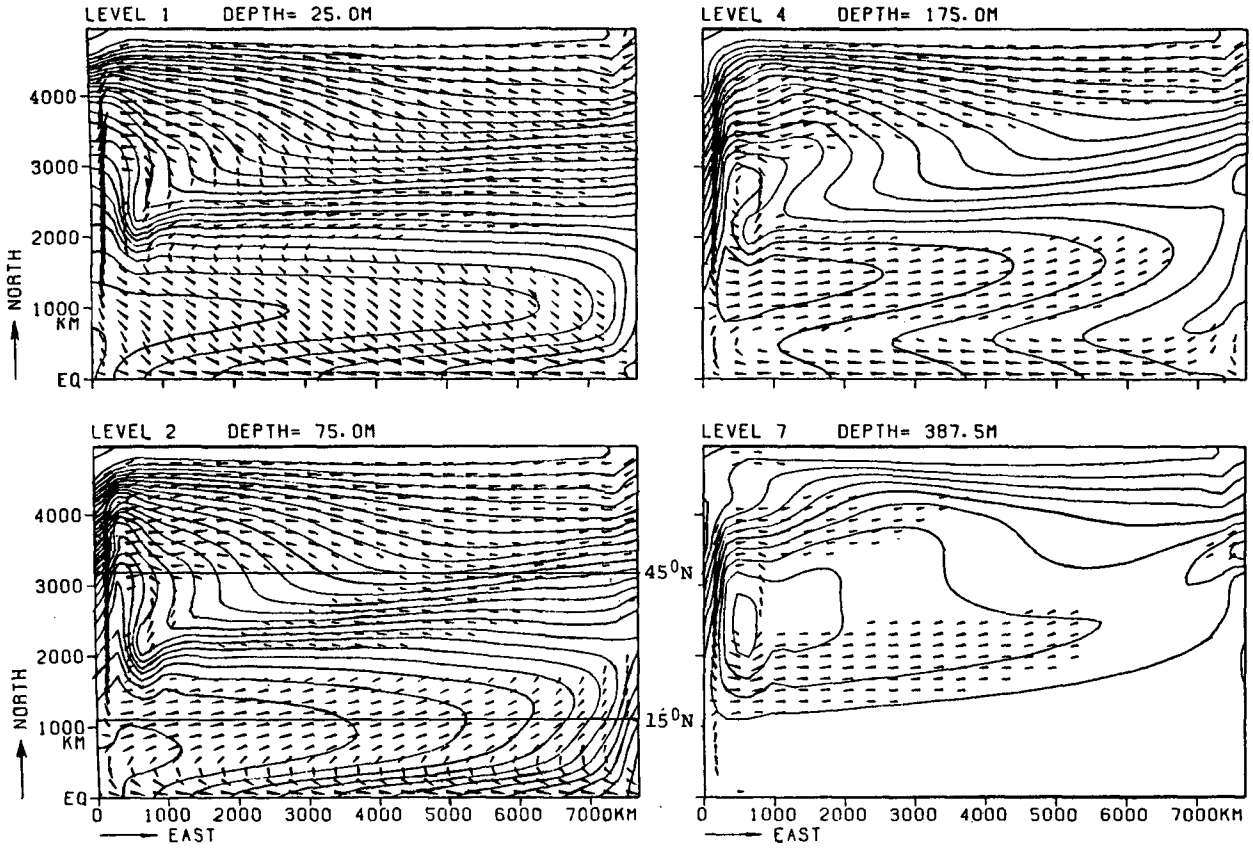

FIG. 2. Horizontal distribution of the density (contours) and currents (wedges, with area proportional to speed) from Takeuchi (1980). Zonal lines drawn at 15 and 45°N mark the boundaries of the model subsequently developed here.

its workings is presented in Section 5. Disagreement along the basin eastern boundary is recorded and explained by the absence in the present, minimal model of the California Current coastal dynamics.

2. Convergence of Ekman transports: An unlikely mechanism

This section investigates and then rejects the convergence of Ekman transports as the primary and sole frontogenetic mechanism at work in the Subtropical Front. It is thus concluded that there should exist another and more fundamental frontogenetic mechanism.

Based on wind data and hydrographic sections, Roden (1975, 1976) pointed out that there is a strong relation between the position of the Subtropical Front and the convergence of the surface Ekman transports. Westerlies to the north generate southward Ekman transports while the Trades to the south generate northward Ekman transports; convergence takes place at the latitude of zero zonal wind, i.e., around 28 to 30°N. However, for this mechanism to be frontogenetic, it is imperative that the water retains somewhat its properties as it flows toward the convergence zone. If the water masses converge at a very slow rate, they adapt to local conditions and by the time they approach the convergence line, they have lost their identity, and no front is formed despite the convergence. Welander (1981) who studied the properties of a thermal front by Ekman convergence, found that there is a critical threshold separating a no-front regime from a sharp-front regime. The essence of that argument is clarified here.

For a meridional velocity equal to the Ekman drift and for a surface heat exchange proportional to the temperature difference between atmosphere and ocean, the heat equation governing the temperature evolution is

$$-\frac{\tau^x}{fH_{\mathrm{Ek}}}T_y = -\frac{k}{H_{\mathrm{Ek}}}[T - T_a(y)],$$

where T and T_a are the oceanic and atmospheric surface temperatures and where H_{Ek} is a typical Ekman depth. In the vicinity of the latitude where τ^x vanishes, one can expand τ^x in a Taylor series and take f as a constant:

$$-\frac{\tau^x_y}{f_0}yT_y = -k[T - T_a(y)],$$

where $y = 0$ corresponds to the latitude where $\tau^x = 0$ and where $f_0 = f(y = 0)$. (Note that this latitude does not necessarily coincide with the latitude where the wind-stress curl is maximum.) For an atmospheric temperature varying linearly with latitude, the particular solution to the above equation is also linear and does not correspond to a front. On the other side, the general solution to the homogeneous equation is of the form

$$T = A|y|^\nu,$$

where ν is given by $\nu = kf_0/\tau_y^x$. The threshold corresponds to $\nu = 1$. Indeed for $\nu > 1$, the temperature gradient at $y = 0$ vanishes (no front), while for $0 < \nu < 1$, the temperature gradient at $y = 0$ is infinite (very sharp front, at the latitude of vanishing zonal wind stress and not at the latitude of maximum wind-stress curl as could be first anticipated). For realistic values of k and τ_y^x (Table 1), ν is found to be 0.6, a value indistinguishable from unity in view of the uncertainty on the parameter values.

The result of this analysis is thus inconclusive. The convergence of Ekman transports may or may not be frontogenetic, depending on the strength of the wind and the vigor of surface heat exchange, which vary with the season and the location. But, there are two other major objections to the likelihood of Ekman convergence as the only frontogenetic mechanism. First, in the western North Pacific, the Subtropical Front is found year-round near 20°N with, at times, a branch as far south as 17°N, while the zonal wind component vanishes around 28°N (Kutsuwada, 1982).

The second objection is more fundamental. In a numerical experiment designed to evaluate the role of Ekman convergence in the Subtropical Gyre, Takeuchi (1980) ran his model with meridional instead of zonal winds, but characterized by the same spatial curl distribution. Aside from minor differences at the uppermost level, his solution was identical to the one obtained with the zonal winds. This experiment leads one to believe that the subsurface dynamics, that include the Subtropical Front and Countercurrent, are not dependent on the actual wind stress but only on its curl distribution. This important result demonstrates that convergence of Ekman transports can hardly be the sole mechanism responsible for the maintenance of the Subtropical Front–Countercurrent structure. Ekman convergence can certainly be favorable to the frontal structure, but it remains to elucidate what is in Takeuchi's model and what could be in nature another and more intrinsic mechanism at work in the central latitudes of the Subtropical Gyre and at depths below the Ekman layer. To conduct such an investigation, a very simple model retaining only the minimal dynamics and thermodynamics is constructed.

TABLE 1. Values assigned to various parameters of the model, in accordance with the North Pacific Ocean.

Earth	Gravitational acceleration	$g = 9.81$ m s^{-2}
	Coriolis parameter (30°N)	$f_0 = 7.3 \times 10^{-5}$ s^{-1}
	Beta parameter (30°N)	$\beta = 2.0 \times 10^{-11}$ m^{-1} s^{-1}
Basin	Zonal extent	$L_1 = 8250$ km
	Meridional extent	$L_2 = 3300$ km
	Active depth	$H = 1000$ m
Dynamics	Maximum wind stress	$\tau_0 = 8.0 \times 10^{-5}$ m^2 s^{-2}
Thermodynamics	Temperature at 1000 m	3.5°C
	Mean atmospheric temperature (30°N)	$T_a(y = 0) = 20$°C
	Atmospheric temperature range	$\Delta T = 20$ deg
	Expansion coefficient	$\alpha = 2.2 \times 10^{-4}$ deg^{-1}
	Surface exchange coefficient	$k = 6.5 \times 10^{-7}$ m s^{-1}
	e-folding depth constant	$a = 5.0 \times 10^{-7}$ m^{-1} s^{-1}

3. A minimal model

In the search for another frontogenetic mechanism besides convergence of Ekman transports, the simplest model possible is constructed, retaining only the fundamental dynamic and thermodynamic processes which are important to the large-scale, long-time, open-ocean behavior of the ocean. The model is three-dimensional, the dynamics are steady, geostrophic, hydrostatic, inviscid and incompressible, and the thermodynamics are reduced to an advective–diffusive heat equation. The governing equations are

$$-fv = -p_x, \tag{1}$$

$$fu = -p_y, \tag{2}$$

$$p_z = \alpha g T, \tag{3}$$

$$u_x + v_y + w_z = 0, \tag{4}$$

$$uT_x + vT_y + wT_z = -(\overline{w'T'})_z, \tag{5}$$

where u, v, w are the eastward, northward and upward velocity components, respectively, p the dynamic pressure (pressure minus basic hydrostatic pressure at rest, divided by a reference density), T an equivalent temperature (here called temperature) which is meant to include all buoyancy effects into one single variable, α the corresponding thermal expansion coefficient and $\overline{w'T'}$ the turbulent vertical heat flux. The dynamics are chosen to be inviscid (both laterally and vertically) since there is no direct interest in the western boundary current (Kuroshio), eastern coastal dynamics (California Current) and in the surface Ekman layer (since one looks for a mechanism other than the Ekman convergence). The model is bounded above by an Ekman layer ($z = 0$), below by a level of maximum penetration of wind-driven currents ($z = -H$), to the east by a vertical wall ($x = 0$) and to the west by a western boundary

region ($x = -L_1$). The depth H is taken equal to 1000 m so that barotropic wind-driven currents are confined in the upper thousand meters of the water column. In reality, the bottom is ~4000 m, but a friction-induced vertical shear exists that renders wind-induced currents smaller with increasing depth. The choice of a thousand meters is the compromise of a frictionless model for the wind-induced currents to have the correct order of magnitude in the upper ocean. Due to the presence of warming at low latitudes and cooling at high latitudes, which are transmitted to the ocean below the Ekman Layer, a vertical heat flux term is necessary in the thermodynamic equation. The parameterization of $\overline{w'T'}$ will be constrained by the most general known, yet particular, solution to the problem. However, the mathematical constraints are physically very plausible. Conceivably, an improvement on the present model would be to include the vertical turbulent fluxes of momentum, $\overline{u'w'}$ and $\overline{v'w'}$ which could, for instance, be related to the heat flux $\overline{w'T'}$ through a dynamic stability criterion. While the vertical heat flux is crucial by providing a heterogeneous vertical stratification and, hence thermal variations below the Ekman layer, Ekman upwelling without diffusion is sufficient to transmit wind effects below the Ekman layer. Another argument in favor of the present approach is the scaling difference between dynamic and thermodynamic penetration depths (Johnson, 1971); the former scales as $E^{1/2}$, the square root of the Ekman number (20–40 m) while the latter scales as $E^{1/4}S^{-1/2}$, a stratification number (100–200 m). The present model includes the second, thicker boundary layer only. Because horizontal diffusion is not crucial, it is omitted. Since the Subtropical Front–Countercurrent structure is found throughout the year (although not always with a pronounced temperature gradient), seasonal and other temporal variations are neglected by the assumption of a steady state. For a comprehensive study of seasonal variations, the reader is referred to Takeuchi (1980).

The boundary conditions are

$$w = -(\tau^x/f)_y \quad \text{at} \quad z = 0, \tag{6}$$

$$\overline{w'T'} = k(T - T_a) \quad \text{at} \quad z = 0, \tag{7}$$

$$w = 0 \quad \text{at} \quad z = -H, \tag{8}$$

$$u = 0 \quad \text{at} \quad x = 0, \tag{9}$$

where $\tau^x(y)$ is a meridionally varying zonal wind stress (divided by a reference density), k a Newtonian heat exchange coefficient ($k \approx 7\ 10^{-7}$ m s^{-1}, according to Haney, 1971) and $T_a(y)$ a meridionally dependent equivalent temperature that decreases with latitude. Condition (7) is one of the simplest ways to incorporate in the model warming at low latitudes and cooling at higher latitudes, as felt in the ocean below the Ekman layer. For the sake of clarity, no meridional component to the wind stress is retained. Its inclusion is rather straightforward. Conditions (6) and (7) typify the dynamic and thermodynamic drives by which the system is forced: Ekman pumping due to the curl of the wind stress and heat exchange induced at its top boundary. If this latter forcing were absent, the model would reduce to an advective model of the oceanic thermocline (Veronis, 1969).

Following the methodology of Welander (1959), one defines a quantity M by $p = M_z$ in terms of which all other quantities are expressed [using (1)–(4)]:

$$u = -\frac{1}{f}M_{yz}; \quad v = \frac{1}{f}M_{xz}; \quad w = \frac{\beta}{f^2}M_x;$$

$$p = M_z; \quad T = \frac{1}{\alpha g}M_{zz}. \tag{10}$$

Eq. (5) can then be written in terms of the function M

$$M_{xz}M_{yzz} - M_{yz}M_{xzz} + \frac{\beta}{f}M_xM_{zzz} = -agf(\overline{w'T'})_z. \tag{11}$$

A solution to this equation is searched for with the form (Needler, 1967 and 1971; Anderson and Killworth, 1979; Clarke, 1982)

$$M = A + B\frac{z}{H} + C\exp\left(\frac{az}{f}\right), \tag{12}$$

where A, B and C are functions of x and y only and a is a pure arbitrary constant. To match the z dependence on the left-hand side, $\overline{w'T'}$ is taken as $k(T - T_a)\exp(az/f)$, which obeys the boundary condition (7). It represents a realistic decay with depth with either warming or cooling throughout the water column in accordance with what occurs at the top ($z = 0$). It should be noted that cooling can thus be felt in the deep waters regardless of stable stratification. Since f/a corresponds to an e-folding depth of variation in the vertical, and since most variations occur in the top 150 m of the water column, a reasonable choice is $a = 5 \times 10^{-7}$ m^{-1} s^{-1} ($f = 7.3 \times 10^{-5}$ s^{-1} at 30°N). With the above expression for M, Eq. (11) reduces to

$$B_xC_y - B_yC_x - \frac{2\beta}{f}B_xC + \frac{a\beta H}{f^2}A_xC = -\frac{\alpha g k f^2 H}{a}(T - T_a). \tag{13}$$

Similarly, the boundary conditions (6) and (8) become

$$A_x + C_x = -\frac{1}{\beta}(f\tau^x_y - \beta\tau^x), \tag{14}$$

$$A_x - B_x + C_x\exp(-aH/f) = 0. \tag{15}$$

It should be noted that the condition $\overline{w'T'} = 0$ at $z = -H$, which has not been imposed to avoid redundancy, is almost met since $\exp(-aH/f) \sim 10^{-3} \sim 0$. Eqs. (13)–(15) form a set of three equations for the unknowns A, B and C. The lateral boundary condition along the eastern wall (9) implies for all z

$$B_y = 0, \quad C = C_y = 0 \quad \text{at} \quad x = 0. \tag{16}$$

The condition $C = 0$ is too restrictive and leads to undesirable singularities. This is a consequence of the particular form of M in (12) which by no means is the most general solution to Eq. (11), although it is the most general *known* analytical solution. The singularities can also be attributed to the lack of appropriate eastern-boundary dynamics (Pedlosky, 1983). Although these dynamics can locally affect the model output along the eastern boundary (e.g., by generating a California Current that bends the Subtropical Front southward), these are deemed irrelevant to the open-ocean minimal model developed here. For the sake of coherency with the above solution, a weaker boundary condition must be imposed. It will be discussed later.

Neglecting the very small exponential in (15), one can integrate (14) and (15) to obtain

$$A - A_0(y) = B - B_0(y) = -C - \frac{x}{\beta}(f\tau^x_y - \beta\tau^x), \tag{17}$$

where A_0 and B_0 are arbitrary functions of y. Since any function of y added to A does not influence the solution in terms of velocity, pressure and temperature, A_0 can be put equal to zero. On the other side, imposing that the vertically averaged zonal velocity vanishes along the eastern wall ($x = 0$) yields $B_y + C_y = 0$, and one can also take B_0 as zero. Using these results to eliminate A and B, one can transform (13) into a single equation for C alone or, better, for the surface temperature $T_s = T(z = 0) = a^2C/\alpha g f^2$:

$$\frac{x}{\beta H}\tau^x_{yy}T_{sx} - \frac{1}{\beta H}\tau^x_y T_{sy} + \frac{\tau^x}{fH}T_{sy} - \frac{a}{f}\left(\frac{\tau^x}{f}\right)_y T_s - \frac{\alpha g\beta}{af}\left(1 - \frac{2f}{aH}\right)T_s T_{sx} = -\frac{ak}{f}(T_s - T_a). \tag{18}$$

This governing equation for the surface temperature $T_s(x, y)$ is the last and key equation that remains to be solved. One recognizes in the first two terms of (18) zonal and meridional advection by the barotropic, nondivergent, Sverdrup flow as would be obtained from a vertically homogeneous, wind-driven model. The third term represents meridional advection by a divergent Ekman return flow (in reaction to the surface Ekman drift, not included). The fourth and fifth terms correspond to vertical heat exchanges due to Ekman pumping and divergence of geostrophic isothermal flow on a beta-plane respectively. The latter of the two is the only nonlinear term in the equation. The term on the right-hand side represents the vertical exchange of heat with the atmosphere. Finally, it should be noted that boundary conditions on T_s must still be imposed. These will be discussed in the next section when it becomes apparent where they must be imposed.

Once T_s has been determined from (18), all other variables can be easily reconstructed:

$$u = \frac{x}{\beta H}\tau^x_{yy} - \frac{\alpha g f}{a^2}F'T_{sy} - \frac{\alpha g\beta}{af}\left[\left(1 - \frac{az}{f}\right)\exp\left(\frac{az}{f}\right) - \frac{2f}{aH}\right]T_s, \tag{19}$$

$$v = -\frac{1}{\beta H}\tau^x_y + \frac{\tau^x}{fH} + \frac{\alpha g f}{a^2}F'T_{sx}, \tag{20}$$

$$w = -\left(1 + \frac{z}{H}\right)\left(\frac{\tau^x}{f}\right)_y + \frac{\alpha g\beta}{a^2}FT_{sx}, \tag{21}$$

$$p = -\frac{x}{\beta H}(f\tau^x_y - \beta\tau^x) + \frac{\alpha g f^2}{a^2}F'T_s, \tag{22}$$

$$T = T_s \exp\left(\frac{az}{f}\right), \tag{23}$$

where $F(z, y) = \exp(az/f) - (1 + z/H)$ and $F' = \partial F/\partial z$. Among the various terms, one recognizes the nondivergent wind-driven Sverdrup flow, the Ekman pumping and its associated meridional Ekman return flow and the baroclinic isothermal flow which is divergent on a beta-plane. The last term in the expression for u is the part of the flow along isotherms that is due to the offset of isotherms with depth resulting from the meridional variation of the vertical e-folding depth a/f.

4. Beta-convergence of isothermal flow: A likely mechanism

The flow along isotherms does not contribute to horizontal advection, but, on a beta-plane, does contribute to vertical advection through the convergence of its meridional component. It is this component of the vertical velocity [second term of (21)] that yields the only nonlinearity in the governing equation (18) for the surface temperature. Quite surprisingly, because of the x derivative, this term resembles a contribution to zonal advection and will be treated as such in what follows.

Equation (18) is a first-order hyperbolic equation that is best solved by the method of characteristics. Because of the nonlinear term, the characteristics are not uniquely defined as curves in the (x, y) plane regardless of boundary conditions. On the contrary,

their slope depends on the evolution of T_s along them, starting from their origin on the boundary. It is thus possible for characteristics to intersect and for a discontinuity in T_s (a thermal front) to be present.

Since the goal of this work is to discern the reason for a discontinuity rather than to reproduce accurately the observed features of the North Pacific Ocean, additional simplifications are in order. Firstly, the Ekman return flow and its associate Ekman pumping through the water column are neglected [third and fourth terms of (18)]. Although these terms are not negligible, they do not change the solution qualitatively. (Results with retention of these terms are not reproduced here.) Second, the zonal wind stress is chosen to obey a sinusoidal

$$\tau^x(y) = \tau_0 \sin(\pi y/L_2)$$

profile where $y = 0$ corresponds to the latitude separating Westerlies and Trades (28–30°N), taken here as 30°N for simplicity. In accordance, the meridional extent of the basin is limited to the latitudes of maximum winds ($y = \pm L_2/2$), which are taken as 15 and 45°N respectively. Finally, the equivalent atmospheric temperature is chosen to decay linearly with latitude from 30°C at $y = -L_2/2$ to 10°C at $y = +L_2/2$ (i.e., 26.5 and 6.5 deg, respectively, for a water temperature at 1000 m of 3.5°C taken as zero in the present formalism).

With the above simplifications, the formalism is reduced to a minimum, and the results can be clearly interpreted. In particular, the tendency toward intersection of characteristics is well illustrated by two particular characteristics which run zonally at the same latitude ($y = L_2/2$, the northern boundary of the basin), one from the west and the other from the east, meeting somewhere in the basin. At that latitude, Eq. (18) becomes

$$-(\lambda x + \mu T_s)T_{sx} = -(T_s - T_N), \tag{24}$$

where $\lambda = \pi^2 f_N \tau_0/\beta Hak L_2^2$ and $\mu = \alpha g \beta(1 - 2f_N/aH)/a^2 k$ with $f_N = f(L_2/2)$ and $T_N = T_a(L_2/2)$; λ, μ and T_N are three positive constants. Along characteristics defined by

$$\frac{dx}{ds} = -\lambda x - \mu T_s,$$

T_s follows the law

$$\frac{dT_s}{ds} = -(T_s - T_N).$$

The solution to this system is

$$\left.\begin{aligned} x &= x_0 e^{-\lambda s} - \frac{\mu T_N}{\lambda}(1 - e^{-\lambda s}) \\ &\quad - \mu \frac{T_0 - T_N}{\lambda - 1}(e^{-s} - e^{-\lambda s}) \\ T_s &= T_N + (T_0 - T_N)e^{-s} \end{aligned}\right\} \tag{25}$$

for a characteristic starting at $x = x_0$ with $T = T_0$. As s tends to infinity, x and T_s tend to equilibrium values $-\mu T_N/\lambda$ and T_N respectively. [This is not a stagnation point in the basin where all velocity components vanish, because the advective velocity in (24) is a fictitious velocity that determines the evolution of temperature along the characteristics. Actual velocity components also include the thermal current.] Since this point lies somewhere to the west of the eastern wall (at about 730 km for the parameter values listed in Table 1), it can be approached by two characteristics, one coming from the eastern wall ($T_0 = T_E$, $x_0 = 0$) and the other originating from the western boundary layer ($T_0 = T_W$, $x_0 = -L_1$). For $T_E = T_W = 16.5$ deg (a zero temperature corresponds to 3.5°C water at 1000 m), the $T_s(x)$ solution is shown in Fig. 3. This analytical solution displays an overshooting of the easterly characteristics, leading to three values for T_s just west of the stabilization point $x = -\mu T_N/\lambda$. Such triple values cannot occur; a consequent temperature discontinuity (front) must be present. It is interesting to determine the threshold (critical value of the surface-exchange coefficient k, for instance) at which overshooting and discontinuity starts to occur. Mathematically, this threshold is defined by requiring an infinite dT_s/dx slope on the easterly characteristic at the stabilization point, i.e., $\lambda = T_N/T_E < 1$. A discontinuity appears for $\lambda > T_N/T_E$ or

$$k < \frac{\pi^2 f_N \tau_0}{\beta Ha L_2^2}\left(\frac{T_E}{T_N}\right) \tag{26}$$

for typical values of the North Pacific Ocean (Table 1); k is typically 6.5×10^{-7} m s^{-1}, while the right-hand side of (26) is about 2.3×10^{-6} m s^{-1}. It is therefore concluded that frontal discontinuities or, at least, large horizontal gradients can be maintained at that latitude. At other latitudes, characteristics do not run exactly zonally, and no definite criterion can be stated. However, it is reasonable to anticipate that, if the above two characteristics intersect, so will many more.

From the inspection of Eq. (18), one notes that the basin is covered by two families of characteristics: one originates from the northern portion of the western boundary, while the other originates from the eastern wall. The front is expected to be situated along the separation line between these two families. To determine the location and shape of this frontal line, one needs to integrate along the characteristics—a task for which one first ought to set boundary conditions on T_s. For the family of characteristics originating from the upper portion of the western boundary, one can take T_s equal to the equivalent atmospheric temperature at the middle of the basin (20°C), arguing that particles leaving the western boundary current are warmer than their environment.

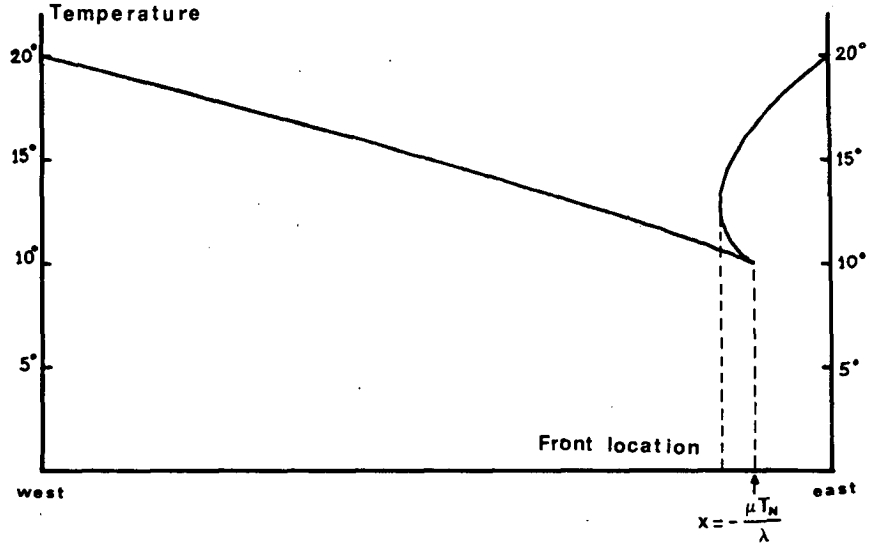

FIG. 3. Zonal distribution of temperature at the latitude of vanishing meridional velocity, as obtained by the method of characteristics. The left branch is influenced by the western-boundary condition, and the right branch by the eastern-boundary condition. Note the triple value near $x = -\mu T_N/\lambda$. Since temperature must be a single-valued function of position, a front must occur in that vicinity.

Bye and Veronis (1980), who studied temperature advection as a passive scalar, obtained a plot showing that the water temperature as it exits the western boundary current is very homogeneous meridionally and close to the equivalent atmospheric temperature across the middle of the basin. For the family of characteristics originating from the eastern wall, the condition yielding a vanishing zonal current is $T_s = 0$ (i.e., 3.5°C) according to (16). This condition leads to singularities which are an artifact of the special solution taken to eliminate the vertical dependence. Implementation of that solution requires a weaker but more realistic condition, and we chose to impose T_s as being uniform along the eastern wall, not zero but equal to the equivalent atmospheric temperature at the middle of the basin $T_a(y = 0)$. Again, the best choice is to include eastern-boundary dynamics (Pedlosky, 1983), but this is too irrelevant to the open ocean, minimal considerations that are developed here.

For these western and eastern boundary conditions, characteristics have been constructed (Fig. 4). Their plot clearly shows that characteristics intersect and that a front runs across the entire basin, south of the latitude of maximum Ekman convergence (30°N) to the west and tilting northeastward. The resulting distribution of the temperature at the base of the Ekman layer ($z = 0$), here called the surface temperature, is presented in Fig. 5. The thermal front is clearly apparent in Fig. 5. Its position agrees with the one of the Subtropical Front in the North Pacific Ocean (see Section 1), except in the eastern portion of the Basin. There, the absence of California Current dynamics do not force the front to meet with the coastal cold-water front generated by this latter current. Agreement with the numerical results of Takeuchi (1980) (see Fig. 2), that also do not include California Current dynamics, strongly suggests that the present simple model retains the essential frontogenetic physics, viz., the beta-plane convergence of the thermal flow.

It should be noted that a much sharper front (greater temperature discontinuity) can be obtained for other values of the parameters (smaller surface heat-exchange coefficient k). Results presented here correspond to the most realistic parameter values and yield a somewhat weak front, like the North Pacific Subtropical Front. The temperature jump across the front in the midocean is evaluated to about 3 deg, which favorably compares to the real ocean.

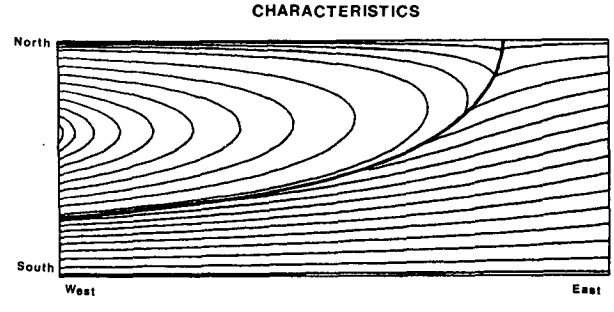

FIG. 4. Sketch of the characteristics for the hyperbolic equation governing the surface temperature. Two independent families intersect along a frontal line. This line corresponds to the line of temperature discontinuity (front) in the solution.

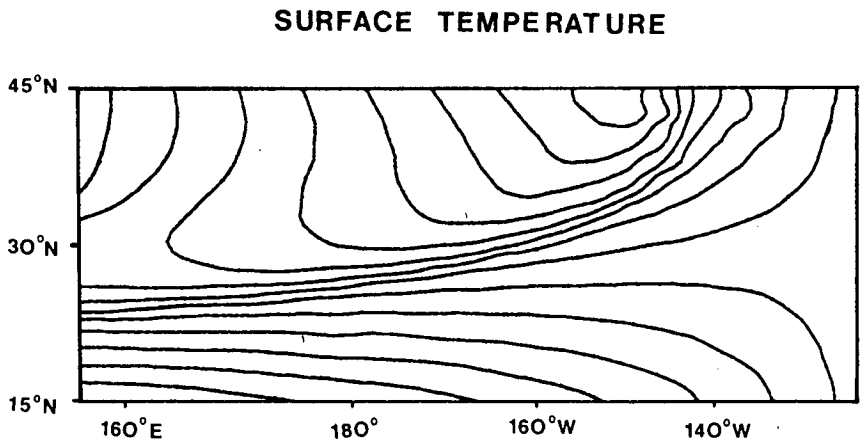

FIG. 5. Surface temperature distribution as obtained numerically by the method of characteristics. Note the front running northeastward across the basin.

From the knowledge of the surface temperature field, all three-dimensional fields can be computed from (19) to (23). Of interest are the horizontal thermal currents at the base of the Ekman layer ($z = 0$), here called surface currents [last terms of (19) and (20)]; these are presented in Fig. 6. Current arrows clearly show an eastward flowing current along the Subtropical Front which is readily identified as the Subtropical Countercurrent. Since only terms of thermal origin have been retained for Fig. 6, one concludes that the Subtropical Countercurrent is confirmed as a geostrophic, gravitational current associated with the frontal horizontal temperature gradient. The vertical dependence of these thermal currents are such that they reverse at depth, yielding no depth-averaged flow. The eastward countercurrent is thus the surface manifestation of the vertical convective-type cell which extends along and below the front. Evidently, due to the depth ratio (~150–1000 m), the underflow is much weaker than the surface current.

Total velocity components are obtained by adding the wind-driven Sverdrup flow to the thermal currents [first terms of (19) and (20)]. These are presented in Fig. 7. This figure shows that the eastward countercurrent overcomes the westward Sverdrup flow, thus remaining identifiable. Since actual thermal currents depend on the frontal width (zero analytically, greater due to numerical smoothing by the computer), actual thermal velocities cannot be accurately estimated. However, the integration across the frontal region provides a good estimation of the total flow along the front, irrespective of its width. Calculations suggest a flow of about 2 Sv (2×10^6 m^3 s), a figure that agrees well with observations and previous numerical experiments (Takeuchi, 1980).

Distribution of the vertical velocity (without Ekman pumping, according to the previously stated simpli-

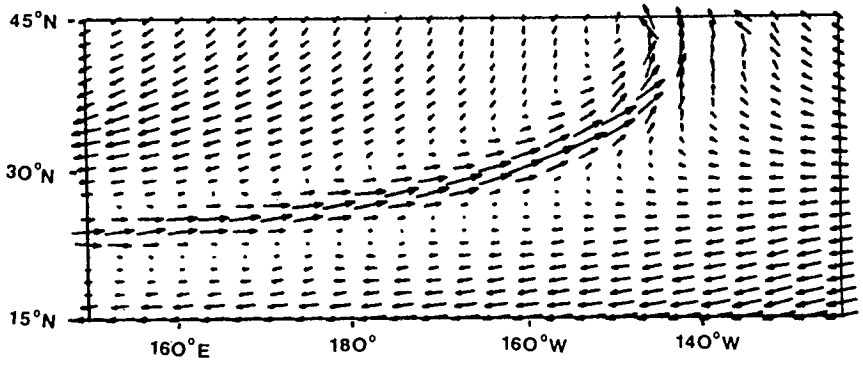

FIG. 6. Surface distribution of the thermal currents as computed from (19) and (20) with the knowledge of the surface temperature field. At depth, these currents reverse.

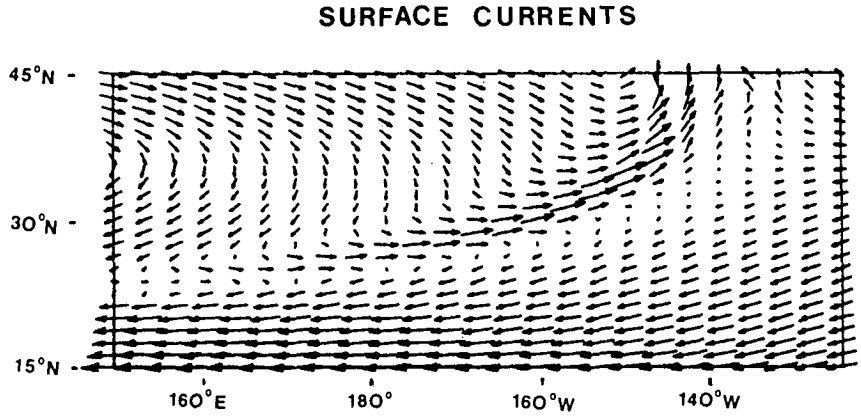

FIG. 7. Surface distribution of the currents (thermally-forced and wind-driven). Note the existence of the eastward flowing Subtropical Countercurrent as a thermal current weakened by the wind-driven circulation. Similarities with the numerical results of Takeuchi (1980) presented in Fig. 2 are evident here.

fication) is displayed in Fig. 8, which shows that the front is a zone of downwelling. This is explained by the negative divergence of the meridional component of the thermal flow which slows down with latitude according to the increase of the Coriolis parameter. It is this downwelling that contributes to the nonlinear term in Eq. (18) and thus to the separation of the basin into two regions of independent origin. This separation of water masses can be better evidenced as one conceptually reconstructs the three-dimensional current pattern. As the surface waters leave the warm western boundary current (western boundary of model), they flow southeastward and eventually southwestward across the basin, meet the front and start flowing northeastward. As they flow along the front without ever crossing that natural boundary, they downwell and participate in an underflow which carries them back into the western boundary region. At the surface, these waters can be identified as the Subtropical Mode Water (Uda and Hasunuma, 1969). On the other side, south of the front, water masses tend to circulate horizontally in a narrow circulation pattern connected to the start of the western boundary current. These can be identified with the Tropical Mode Water (Uda and Hasunuma). The two water modes are clearly separable near the surface, justifying different names. Due to the presence of the southward California Current in the eastern basin, the Tropical Mode Water is not found as far north as Fig. 5 indicates.

Finally, by sake of completion, the distribution of the surface heat flux is presented in Fig. 9, which shows that waters north of the front are anomalously cold and are being warmed by the atmosphere. In addition to their warm origin in the western boundary current, these waters have been appreciably cooled by upwelling of colder water through the process of divergence of meridional thermal flow on a beta-plane.

Inclusion of the previously neglected terms [third and fourth terms of Eq. (18)] yields qualitatively similar results. Differences include a southward shift

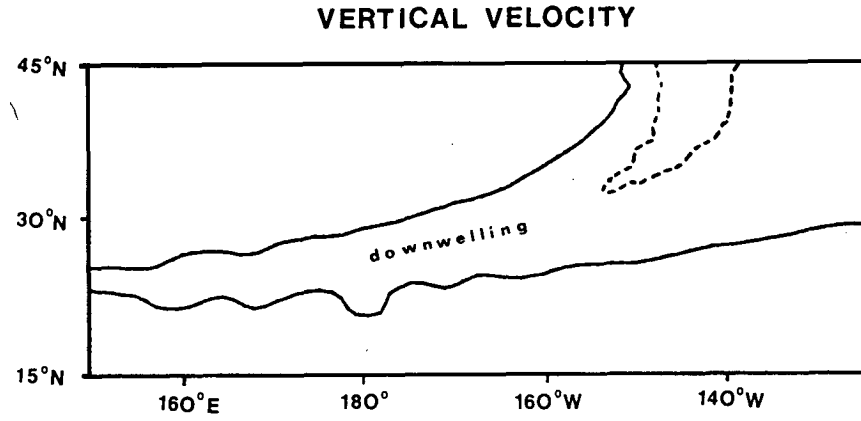

FIG. 8. Distribution of vertical velocity at $z = -f/a$, i.e., near the depth of maximum value. The Subtropical Front is associated with downwelling required by the convergence of thermal currents flowing northward on a β-plane.

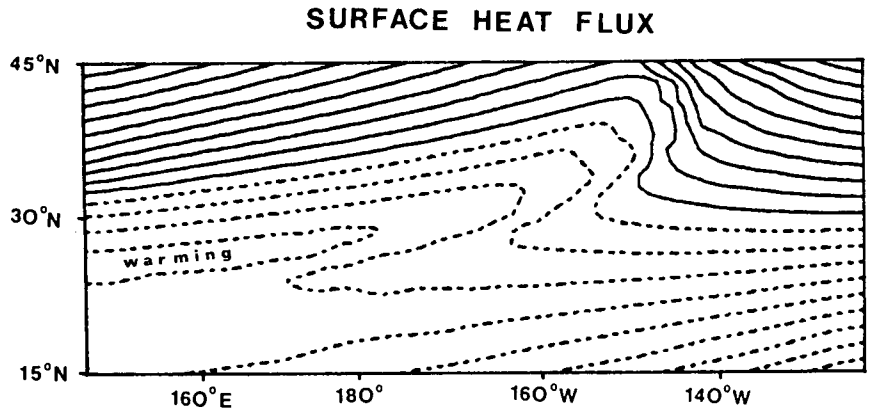

FIG. 9. Distribution of surface heat flux (warming in dashed lines, cooling in continuous lines).

of the latitude where two characteristics run perfectly zonally, a slight weakening of the front by divergent Ekman return flow, and a blurring of the beta-plane induced downwelling by Ekman pumping. Although these additional processes are present in nature, their absence in the previous results has helped, by a process of elimination, to identify a likely frontogenetic mechanism.

5. Conclusions

This work undertook the task of identifying a frontogenetic mechanism that could be responsible for the existence and maintenance of the large-scale Subtropical Front such as the one observed in the North Pacific Ocean. Based on several arguments, mainly that the flow under the Ekman layer is driven by the wind-stress curl rather than by the stress itself, it was first concluded that convergence of Ekman transports to the right of the winds could not be the sole process responsible for the front.

To elucidate a more plausible but less obvious mechanism, it was first observed that numerical models capable of reproducing an eastward countercurrent, such as the one associated with the Subtropical Front (Haney, 1974; Takeuchi, 1980), were strongly influenced by the presence of a surface heat flux with the atmosphere and the role of thermal currents. Therefore, incorporation of temperature as an active scalar was judged crucial, and a simple steady, yet three-dimensional, model was constructed. Forcings are of two natures: Ekman pumping proportional to the wind-stress curl and surface heat exchange depending on a latitude-dependent equivalent atmospheric temperature. The velocity field has corresponding wind-driven and thermally-induced components. After elimination of the vertical dependence, the problem is reduced to a single, first-degree hyperbolic nonlinear equation for the temperature at the base of the Ekman layer. The nonlinearity is such that for the parameter values of the problem, characteristics intersect, and a temperature discontinuity is to be expected. This corresponds to a thermal front which is readily identified to the Subtropical Front by having approximately the same position and the same properties.

The advantage of the simple model is that it permits backward tracing of the process responsible for the existence of the front. The temperature discontinuity is explained by intersecting characteristics, a phenomenon attributable to the nonlinear term in the governing equation. In turn, this term is traced to the vertical velocity induced by the convergence of geostrophic thermal flow on a beta-plane. Since $w \sim \beta z T_x / f^2$, positive (negative), divergence occurs if the thermal flow has a southward (northward) component. Due to the presence of an eastern obstacle, the thermal flow must have a meridional component. If this latter is directed southward ($T_x < 0$), it brings divergence, smooth temperature variations by spreading of isotherms, slow thermal flow, adjustment to the atmospheric conditions and a resulting zonal temperature distribution ($T_x = 0$), i.e., a contradiction. The result is that the meridional component ought to be directed at least slightly northward, bringing downwelling, convergence, large temperature gradients, fast thermal flow, the possibility of finding anomalously warm water and, thus, a front. The convergence zone acts as a barrier on each side of which water masses flow and sink while remaining identifiable as of different origin. The front is the expression of that water mode separation.

The above mechanism, which relies on the wind-stress curl rather than the stress itself and mostly on thermally induced currents, is able to explain some general features of the Subtropical Front. It is thus conjectured that it could be the primary mechanism responsible for the existence and maintenance of the Front. However, since meridional convergence of Ekman transports strengthens the Front near the surface, it remains debatable how both mechanisms measure up in the upper ocean. In addition to the

two previously cited frontogenetic mechanisms, it should not be precluded that a third one may be present, such as a deformation field. However, no existing theory has yet shown how the dynamics of the North Pacific Ocean could set up a deformation field that could lead to frontal formation at midlatitudes.

A more faithful reproduction of the Subtropical Front than discussed can be obtained by including additional physical processes such as lateral diffusion of heat, western- and eastern-boundary dynamics and surface Ekman drift. Previous numerical models (Haney, 1974; Takeuchi, 1980) have already accomplished this task with, as cost, the inability to explain why some observed and reproduced features occur. On the counterpart, the extremely simplified analytical approach developed here elucidates, with a minimum of physics, a likely mechanism at work in the central latitudes of the Subtropical Gyre that can cause frontogenesis and an eastward countercurrent. Finally, it should be noted that the frontogenetic mechanism (presence of a nonlinear term in the governing equation) is present irrespective of any boundary condition. The proposed mechanism is thus quite robust.

Acknowledgments. The author is indebted to Drs. James J. O'Brien and K. Takeuchi for numerous suggestions about this work. Support was provided by the Office of Naval Research.

REFERENCES

Anderson, D. L. T., and P. D. Killworth, 1979: Non-linear propagation of long Rossby waves. *Deep-Sea Res.*, **26,** 1033–1049.

Bye, J. A. T., and G. Veronis, 1980: Poleward heat flux by an ocean gyre. *Dyn. Atmos. Oceans,* **4,** 101–114.

Clarke, A. J., 1982: The dynamics of large-scale, wind-driven variations in the Antarctic circumpolar current. *J. Phys. Oceanogr.*, **12,** 1092–1105.

Haney, R. L., 1971: Surface thermal boundary condition for ocean circulation models. *J. Phys. Oceanogr.*, **1,** 241–248.

——, 1974: A numerical study of the response of an idealized ocean to large-scale surface heat and momentun flux. *J. Phys. Oceanogr.*, **4,** 145–167.

Hasunuma, K., and K. Yoshida, 1978: Splitting of the Subtropical Gyre in the western North Pacific. *J. Oceanogr. Soc. Japan,* **34,** 160–171.

Johnson, J. A., 1971: On the wind-driven circulation of a stratified ocean. *J. Mar. Res.*, **29,** 197–213.

Kenyon, K. E., 1981: A shallow northeastward current in the North Pacific. *J. Geophys. Res.*, **86C,** 6529–6536.

Kutsuwada, K., 1982: New computation of the wind stress over the North Pacific Ocean. *J. Oceanogr. Soc. Japan,* **38,** 159–171.

Needler, G. T., 1967: A model for thermocline circulation in an ocean of finite depth. *J. Mar, Res.*, **25,** 329–342.

——, 1971: Thermocline models with arbitrary barotropic flow. *Deep-Sea Res.*, **18,** 895–903.

Pedlosky, J., 1983: Eastern boundary ventilation and the structure of the thermocline. *J. Phys. Oceanogr.*, **13,** 2038–2044.

Roden, G. I., 1972: Temperature and salinity fronts at the boundaries of the Subarctic–Subtropical transition zone in the western Pacific. *J. Geophys. Res.*, **77,** 7175–7187.

——, 1975: On North Pacific temperature, salinity, sound velocity and density fronts and their relation to the wind and energy flux fields. *J. Phys. Oceanogr.*, **5,** 557–571.

——, 1976: On the structure and prediction of oceanic fronts. *Nav. Res. Rev.*, **29**(3), 18–35.

——, 1980a: On the subtropical frontal zone north of Hawaii during winter. *J. Phys. Oceanogr.*, **10,** 342–362.

——, 1980b: On the variability of surface temperature fronts in the western Pacific, as detected by satellite. *J. Geophys. Res.*, **85C,** 2704–2710.

Schroeder, E. H., 1965: Average monthly temperatures in the North Atlantic Ocean. *Deep-Sea Res.*, **12,** 323–343.

Takeuchi, K., 1980: Numerical study of the Subtropical Front and the Subtropical Countercurrent. Doctoral dissertation, Ocean Res. Inst., University of Tokyo, 45 pp.

Uda, M., and K. Hasunuma, 1969: The eastward Subtropical Countercurrent in the western North Pacific Ocean. *J. Oceanogr. Soc. Japan,* **25,** 201–210.

Veronis, G., 1969: On theoretical models of the thermocline circulation. *Deep-Sea Res.*, **16**(Suppl.), 301–323.

Welander, P., 1959: An advective model of the ocean thermocline. *Tellus,* **11,** 309–318.

——, 1981: Mixed layers and fronts in simple ocean circulation models. *J. Phys. Oceanogr.*, **11,** 148–152.

Yoshida, K., and T. Kidokoro, 1967a: A subtropical countercurrent in the North Pacific—An eastward flow near the Subtropical Convergence. *J. Oceanogr. Soc. Japan,* **23,** 88–91.

——, and ——, 1967b: A subtropical countercurrent (II).—A prediction of eastward flows at lower subtropical latitudes. *J. Oceanogr. Soc. Japan,* **23,** 231–246.